연구논문집 제29권 제1호 pp. 37~46 울산과학대학
Journal of Research Vol. 29, No. 1, pp. 37~46, 2002
Ulsan College

실리콘을 델타도핑하여 만든 2차원 전자가스층이 포함된 다중양자우물 나노구조의 청색발광다이오드 제작

김 근 주
전기전자학부

<요 약>

청색 발광 다이오드의 다중 양자 우물 구조를 사파이어 기판 위에 유기금속 화학기상 증착법으로 성장시켰다. 증착된 시료는 InGaN/GaN의 5주기 다중 양자 우물구조이며 양자우물 발광 활성층 근처에 실리콘 델타도핑을 하였다. 전기적 및 광학적 특성을 양자효율과 다이오드의 동적 저항의 관점에서 조사하였다. 청색 발광 다이오드의 동작전압과 동적 저항은 실리콘 델타 도핑층을 포함시킴으로써 감소함을 확인하였다.

The inclusion of silicon delta-doped two-dimensional electron gas layer on multi-quantum well nano-structures of blue light emitting diodes

Kim, KeunJoo
School of Electricity and Electronics

<Abstract>

The multi-quantum well structures of blue light emitting diodes were designed and grown on sapphire substrates by using metal-organic chemical vapor deposition. Sample were deposited for 5 periods InGaN/GaN multi-quantum well layers and Si delta doped layer was included in the vicinity of quantum well active layer. The electrical and optical properties were investigated in terms of quantum efficiency and dynamic resistance behaviors. The forward operating voltage and dynamic resistance of blue light emitting devices were decreased by the inclusion of the Si delta doped layer.

Key words : Blue LED, Multi-quantum well, Si delta doping, 2DEG

Ⅰ. Introduction

Recently, light-emitting diodes (LEDs), fabricated from III-V nitride compound semiconductors, for the blue range of visible light wavelengths have been intensively investigated[1,2]. The blue LEDs were fabricated for high output power or high external quantum efficiency for the p-n junction diodes[3,4], double hetero-junction (DH) diodes[5], single quantum well (SQW) structure[6] and

multi-quantum well structures (MQW)[7].

For the DH and the quantum well structures, InGaN layers have been utilized for the active layer and the AlGaN layer for the cladding layer. The quantum well structures in the active region of LEDs provide the devices with high output power and narrow band emission[6].

For the uniformly distributed current density from p-electrode, the Ni/Au light transmitting layer was introduced[8]. For the electron path from the n-type contact layer to the active layer, the undoped GaN layer has been utillized as for current distribution pair [9]. It is valuable to improve the undoped layer which plays a blocking barrier as well as charge spreading layer.

In this work, a two-dimensional electron gas layer upon the n-type contact layer has been introduced in the vicinity of the quantum well structure by the implementation of a delta doping technique. The fabricated LED grown with 5-periods multi-quantum well active layer provides the relatively enhanced output power and quantum efficiency. Furthermore, there is an evidence on the relative decrease of the dynamic resistance.

II. Experimental

GaN films were grown by the metal-organic chemical vapor deposition (MOCVD) method in the vertical mode of reactor. The epitaxial growths of quantum well structures were carried out in the low pressure of 200 Torr at the temperature of 780℃. Sapphire wafer of C(0001) basal plane with a two-inch diameter was used for substrate. Trimethylgallium (TMGa), Trimethylindium (TMIn), ammonia (NH_3), silane (SiH_4) and bis-cyclopentadienyl magnesium (Cp_2Mg) were used as Ga, In, N, Si and Mg sources, respectively.

The substrate was heated to 1030℃ in a stream of hydrogen and then, the substrate temperature was lowered to 490℃ to grow the GaN nucleation buffer layer. The thickness of the buffer layer was about 300Å. The growth temperatures of the fabrication process for sample K3 is shown in Fig 1. The main flow rates of H_2, NH_3 and TMGa were kept at 7.3 slm(liter/min), 7.3 slm and 103μ-mol/min, respectively. The n-type GaN film with a thickness of 2.2 ㎛ was grown for 50 min by flowing SiH_4 gas at the flow rate of 1.11 nano-mol/min.

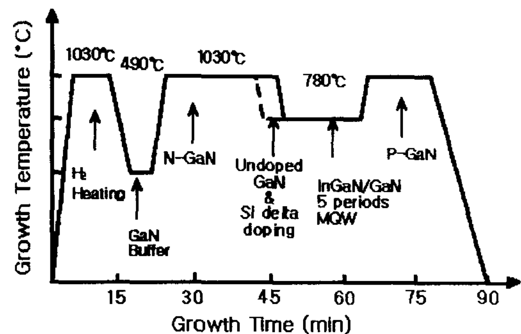

Fig 1. Growth temperature distribution on various film layers. After growth of n-type GaN, n-type GaN layer, undoped GaN layer and Si delta doping in the undoped layer were introduced in samples K1, K2 and K3 , respectively.

For samples K1, K2 and K3, the same Si doped n-type GaN film, the undoped GaN film and the undoped GaN with the inclusion of Si delta doping were added with the thickness of 150Å for the same growth temperature of n-type GaN film. For the Si delta doping, after growth of the undoped GaN layer with a thickness of 100Å, the TMGa source was interrupted to be switched off to form the Si delta doped two dimensional electron gas (2DEG) layer during the intermediate interval of 20 sec.

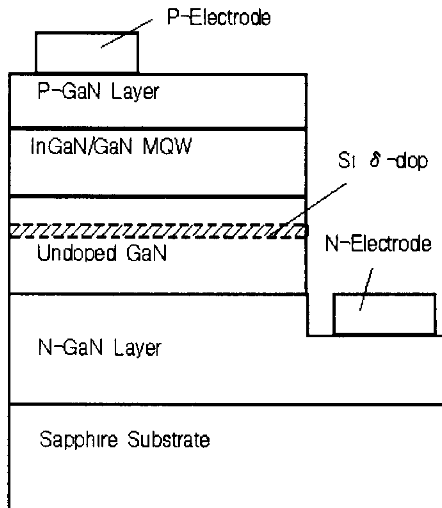

Fig 2. The device structure of the 5 periods MQW InGaN/GaN LED for K3 sample. K1 sample with the n-type doped layer instead of undoped layer was grown for a reference and K2 sample has only undoped layer. During the Si delta doping in the sample K3, the TMGa source was switched off.

Figure 2 shows the LED structure of the sample K3, including an undoped GaN layer with 2DEG layer. The 5 periods InGaN/GaN MQW structures with well widths of 25Å and barrier widths of 50Å were grown at the temperature of 780℃.

Furthermore, the single layer structures such as a Si doped n-type GaN film, a Si delta doped layer in undoped thin GaN layer on n-type GaN film, and a Mg doped p-type GaN film were grown for the structural evaluations of physical properties. From Hall effect measurement, the carrier concentrations of n- and p-type contact layers were evaluated to the values of 6.0×10^{18} and $2.2\times10^{17}/cm^3$, which are corresponding to the electron quasi-Fermi level of 34 meV from conduction band edge and to the hole quasi-Fermi level of 0.13 eV from valence band edge, respectively. The undoped GaN layer and the Si delta doped layer show the carrier concentrations of 5.3×10^{16} and $8.6\times10^{19}/cm^3$, respectively. This indicates that the Si delta doping may provide the formation of two-dimensional electron gas layer.

For the LED fabrications, the surface of the p-type GaN layer was partially etched until the n-type contact layer was exposed. The etching process was performed by the implementation of an inductively coupled plasma (ICP) of Cl_2 etching gas. For metal Ohmic contacts, the Ni/Au and Ti/Al metal layers were evaporated onto the p-type GaN and n-type GaN contact layers by utilizing an e-beam evaporator, respectively. For chip separation, the back lapping process of sapphire wafer to a thickness of 0.08 mm can be achieved in home-made lapping system. Finally, by

scribing the surface of wafer along the scribing line by diamond tip and by breaking wafer with knife edge, LED wafers can be separated into square dies with the dimension of 0.35×0.35 mm^2. These dies were attached on lead frame and then were molded on TO-18 LED lamps as shown in Fig 3. The chips for K1, K2 and K3 samples of 5 periods InGaN/GaN MQW structures were prepared with the only difference of Si doped n-type GaN layer, with undoped GaN layer and with undoped GaN layer including 2DEG layer, respectively.

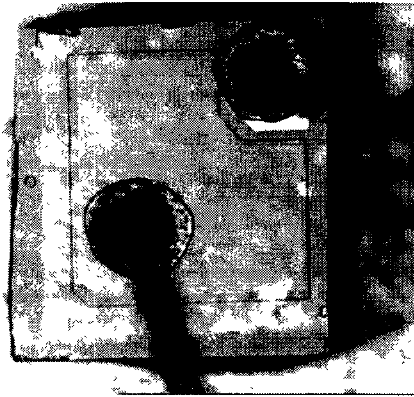

Fig 3. TO-18 molded blue LED chip. The chip was fabricated by the implementation of processes: the n-type contact layer etching, the Ohmic contact metal deposition, the sapphire back-lapping, the scribing and breaking, and the wire bonding.

Ⅲ. Results and Discussion

The Ohmic property of p-GaN and Ni/Au alloy was analyzed in terms of the annealing temperature on the p-type contact layer as shown in Fig 4. The resistance is not monotonically decreased with increasing annealing temperature.

The optimum annealing temperature is about 450℃. As increasing the temperature, the reaction of p-GaN and Ni/Au alloy enhances the linearity of Ohmic character and surface built-in potential barrier decreases. However, the linearity is still required to be improved indicating the limitation of the reduction of work function. The further increase of the temperature provides the deteriorated quality of current-voltage (I-V) characteristic.

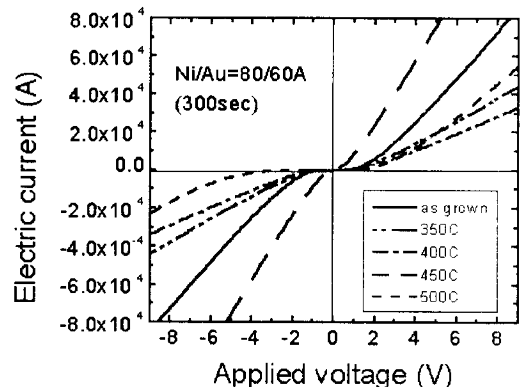

Fig 4. I-V characteristics on the p-type ohmic contact of Au/Ni alloy and GaN thin film with the alloy thicknesses of 80/60Å for various annealing temperatures, respectively. The optimal annealing temperature was picked up at 450℃. However, there still exists a tiny Schottky built-in potential

According to Ishikawa et al. [10], Ni/Au provides the lowest resistance for the annealing temperature of 500℃ among their samples of Ta, Au, Pt, Ni metals and Ni/Au

alloy. They concluded the improvement of the current inject is due to the removal of the surface contamination layer and the reaction between the GaN and the contact metals.

The electrical properties on the Mg related defect in the p-type GaN layer were extensively investigated in terms of the p-type transport channel induced by the deep hole trap centers[11,12].

Furthermore, the wide band gap of GaN provides the quasi-Fermi level close to valence band edge with the energy interval of about 0.13 eV at a hole carrier concentration of $2.2\times10^{17}/cm^3$ [13].

Therefore, the Ohmic character in p-type contact layer is very difficult to achieve the reduced operating voltage with the limited work functions of various metals.

The reactive interface of metal- semiconductor contact by thermal annealing is the alternative method to achieve Ohmic contact.

The I-V characteristics of samples K1, K2 and K3 are shown in Fig 5. The forward voltages are 6.30, 4.20 and 4.18 V at 20 mA, respectively. Usually, the large static resistance is attributed to Ohmic contact property and the large dynamic resistance to device structure.

The static and dynamic resistances are defined as an average resistance in the current interval from 0 to 20 mA and an instantaneous resistance at an operating current of 20 mA, respectively. Samples K1, K2 and K3 show 325, 210 and 209 Ω for static resistances and 137, 25 and 18 Ω, for dynamic resistance, respectively. The K1 sample without the undoped GaN layer shows the different I-V behavior to K2 and K3 samples, which have the undoped GaN layer in the vicinity of the quantum well. The large static and dynamic resistances in the sample K1 indicates that both the contact property and structural property were not optimized and the abnormal diode character in I-V curve was shown. At low voltage application at 3 V, the sample K1 shows the larger value of current to compare to other samples, indicating the leakage through a focused current density at a least path. However, the K2 and K3 samples show normal I-V curves of diodes. The Si delta doping effect is not significant but there is a little change on the dynamic resistance. The shape of I-V curves in

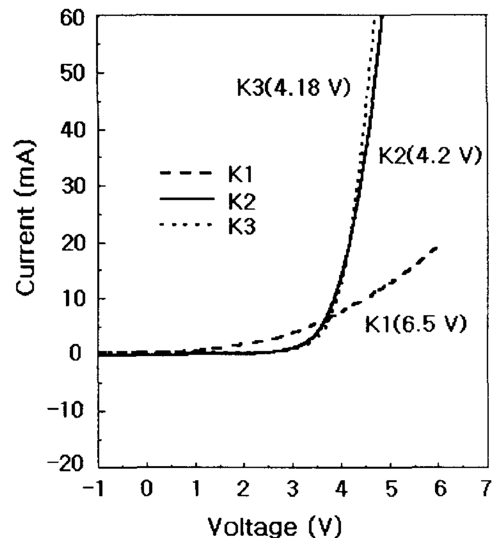

Fig 5. Typical I-V characteristics of 5 periods MQW InGaN/GaN LEDs. The operating voltages are measured to the values of 6.3, 4.2 and 4.18 V at 20 mA for the samples K1, K2 and K3, respectively.

sample K2 and K3 samples provides the similar energy barrier for the applied bias to be turned on. This implies that the resistive p-GaN layer is dominant to reduce the static and dynamic resistances in I-V characteristics. However, there is still a tiny change on dynamic resistance by the introduction of the Si delta doping.

Let us analyze the energy diagram of a multi-layered structure including Si delta doping layer at forward bias as shown in Fig 6. The 2DEG structure can supply electron into quantum wells through the process of quantum tunnelling. The electron wave function in delta potential is strongly correlated with quantum well and the voltage bias enhances electron tunnelling. This 2DEG layer can also spread the electron density to be uniformly recombine with holes in whole area. The undoped GaN layer including 2DEG plays a role of a space charge region where

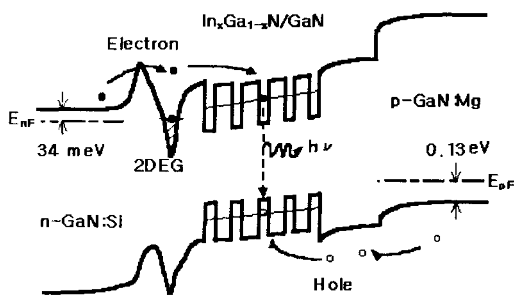

Fig 6. Schematic energy band diagram of 5 periods MQW InGaN/GaN LEDs with the inclusion of the Si delta doping. The delta doped layer reduces strain induced band distortion and serves as an electron spreading layer.

tunnelling, injection and recombination can be occurred. And also, the injection and the recombination can be occurred in QW active layer. However, the tunnelling process is mainly occurred in the space charge region and radiative recombination is in the QW active layer.

The bright field image of transmission electron microscope (TEM) on InGaN/GaN multi-quantum well nano-structures is shown in Fig 7. There exist large misfit dislocations originated from the surface of sapphire wafer. The GaN quantum barrier and the quantum well are shown as a narrow band and a line, respectively.

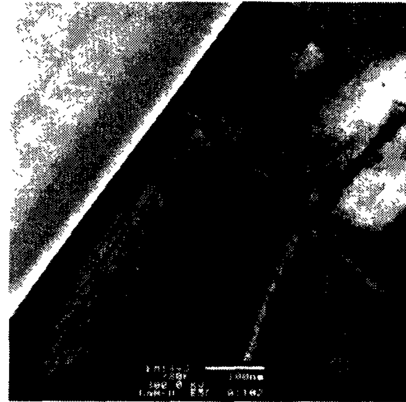

Fig 7. Bright field TEM image of InGaN/GaN quantum well nano-structures.

Figure 8 shows the high resolution TEM image on the nano-structure of active layer of electron-hole recombination. The widths of GaN quantum barrier and InGaN quantum well are 10 and 2 nm, respectively. The contrast image in quantum wells attributed to the stress concentration and indicates that the In corporation is

not uniform and microscopic InN phase separation can be occurred.

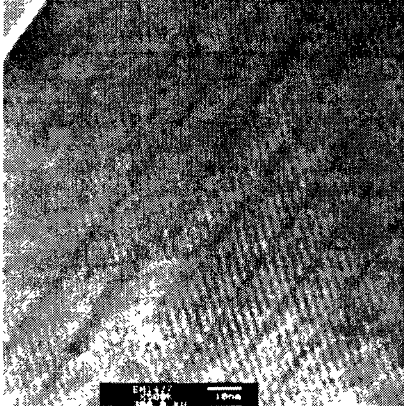

Fig 8 High resolution TEM image of InGaN/GaN quantum well nano-structures.

The photoluminescence (PL) intensity is strongly correlated with the space charge regions where electron can be supplied on optical pumping. Under the voltage bias, the electroluminescence (EL) intensity is originated from effective radiative recombination when both carrier types are injected to the active QW layer. At high currents, some of the voltage will drop across the adjacent undoped layers and some recombination will occur there.

Figure 9 shows the PL spectra from LED structures. The PL data show strong quantum well emission with a narrow line width, and the several multi-band peaks originated to the optical interference due to a film thickness effect. The radiativerecombinations from MQWs provides optical energies of 2.57(482), 2.58(480) and 2.63 eV (471 nm) for K1, K2 and K3 samples, respectively. The PL signals are intense in samples of K1 and K3 where the samples are normally n-type doped without undoped layer and Si-delta doped within an undoped layer, respectively. The 2.2 eV-yellow band from n-GaN layer is negligible. The weak signals both from Mg defect related PL band of p-type GaN at 3.0-3.1 eV and from the excitonic level of GaN at 3.4 eV are shown

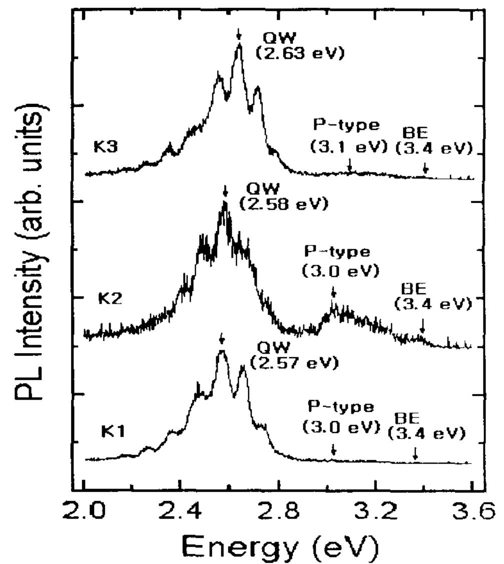

Fig 9. PL spectra on 5 periods MQW InGaN/GaN LEDs. The QW related blue emissions at the energy of 2.63 eV is very intense in Si delta doped sample K3 to compare to the sample K2 including undoped GaN layer The intensity of the regularly n-type doped sample K1 is strongest, indicating that the n-type space charge region is correlated with the optical pumping.

The MQW structures with the well widths of 25Å and the barrier widths of 50Å showed good luminescence quality

The PL peak energy of 2.57-2.63 eV provides the Indium (In) composition range of x=0.27-0.29 with the correction of stress effect into empirical bowing factor[8,14]:

$$E_g(x) = xE_g(InN) + (1-x)E_g(GaN) - bx(1-x), \quad (1)$$

where, $E_g(x)$ represents the band-gap energy of $In_xGa_{1-x}N$, $E_g(InN)$ and $E_g(GaN)$ represent the band-gap energies of compound InN and GaN, respectively, and b is the bowing parameter[15]. For the energy band gap values, $E_g(InN)$ was 1.95 eV, $E_g(GaN)$ 3.40 eV and b 1.00 eV. The PL intensity of samples K1 where the QW contacts with n-type interfacial layer without space charge region is strongest and then that of the sample K2 with an undoped layer of space charge region is weakest. The undoped layer in the vicinity of the MQW is very strained which can distort the MQW. This internal strain-induced piezoelectric field can cause spatial separation of electrons and holes reducing the oscillator strength and luminescence intensity[16].

Figure 10 shows the EL spectra from LED lamps. The peak wavelengths and the full widths at half-maximum(FWHM) at 20mA are 460-468nm and 75-105nm, respectively. Furthermore, the deep level emission was observed at 780nm. The EL peaks for samples K1, K2 and K3 are located at the energies of 2.65(468), 2.70(460) and 2.66eV (466nm), respectively. The peak energy differences between the PL spectra and the EL spectra are about 80, 120 and 30 meV for the samples K1, K2 and K3 grown with spatial charge regions of a normally n-type doped

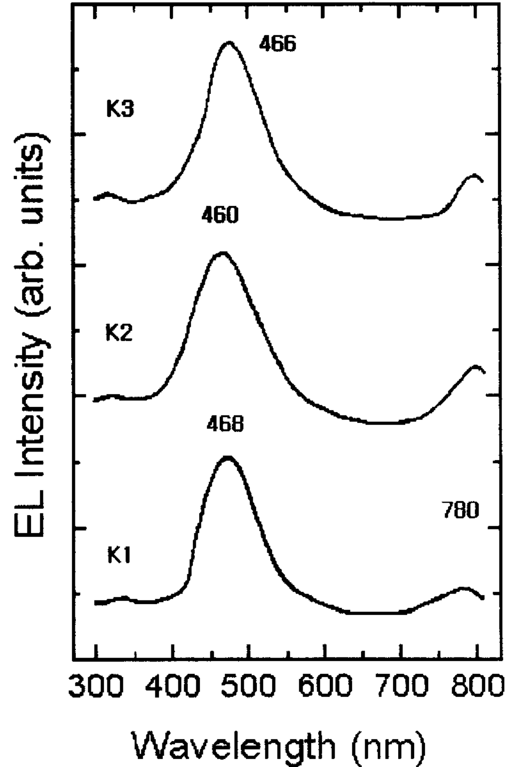

Fig 10. EL spectra on 5 periods MQW InGaN/GaN LEDs measured at the operating current of 20 mA. The input powers for samples K1, K2 and K3 were 130, 84 and 83.6 mW, respectively.

layer, an undoped layer and an undoped layer with the inclusion of a delta doped layer, respectively. This indicates that an n-type doping effect reduces the strain distortion at InGaN/GaN MQW interface The more ionic bond nature of GaN than any III-V compound semiconductors shows the ionicity of I=0.34 estimated from the

empirical formula,

$$I = 0.166x + 0.12x^2 - 0.024x^3, \quad (2)$$

where, x is the difference of electronegativities between Ga and N. This strong ionicity provides a strain induced piezoelectric effect and attributes to a severly distortions of the interfacial band structure and active InGaN/GaN MQW band. This internal field effect due to the more ionic character of GaN-based crystals was reduced by the introduction of the Si delta doping in the vicinity of the QW structure.

The external quantum efficiency can be simply defined by the ratio of light output power to electrical input power. For fabricated MQW LED lamps, the optical outputs at forward currents of 20 mA were measured to the values of 2.1, 1.8 and 2.0 mW, providing the quantum efficiencies of 1.6, 2.14 and 2.4% for the samples of K1, K2 and K3, respectively. The further optical power emissions of LEDs have been measured as a function of dc current as shown in Fig 11.

From these luminescence-current (L-I) curves, the sample K1 shows the saturated power at 6.5 mW under the dc current of 100 mA. This saturation indicates that the leakage current affects on the non-radiative recombination. However, the stable high power emissions were shown in the samples K2 and K3. The Si delta doping effect also did not affect on the carrier overflow, which cause the reduction of the optical output power Within the quality of sample growths, the Si delta doping effect sheds a light on the improvement of the blue LEDs. Although the sample K1 shows the turn on voltage of 1.5 V, the operating voltage at 20 mA is very much elongated and it gives low quantum efficiency. The normal structure of K1 sample without the inclusion of undoped GaN layer provides resistive transport channel for carriers in the LED structure. Both samples K2 and K3 with the undoped GaN layers show the normal diode character in I-V curve and Si delta doping effect can improve LED physical properties of the dynamic resistance, the internal strain distortion and the external quantum efficiency.

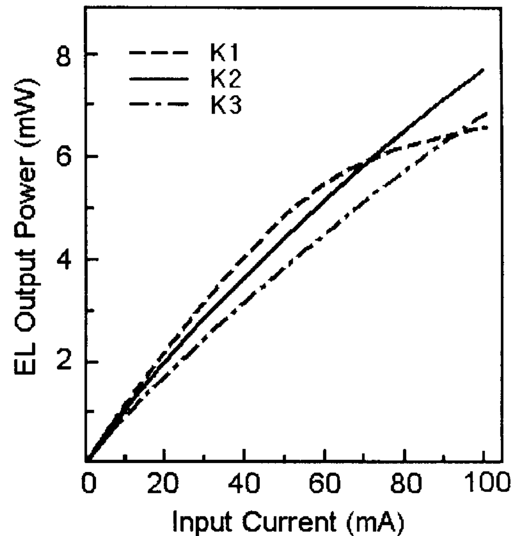

Fig 11. Typical L-I characteristics of 5 periods MQW InGaN/GaN LEDs under dc current. The sample K1 shows saturated output power at a current of 100 mA.

Ⅳ. Summary

The fabricated LEDs grown with the 5 periods multi-quantum well active layer exhibit output power of 2.1, 1.8 and 2.0 mW at forward currents of 20mA providing the efficiencies of 1.6, 2.14 and 2.4% for the samples of K1, K2 and K3, respectively. The dynamic resistances were evaluated to the values of 137, 25 and 18Ω for samples K1, K2 and K3, respectively. The undoped layer as a charge spreading layer is important for the preservation of diode characteristics. The inclusion of two dimensional electron gas layer in the vicinity of the active layer rendered a small increase in output power and quantum efficiency. As a concluding remark, the inclusion of Si delta doped layer within the undoped space charge region improve LED properties for the charge spreading and the electron tunnelling into QW layer.

Acknowledgement

This work was supported through the Korea Research Foundation Grant (KRF-99-E00198).

References

1. S. Nakamura, M. Senoh, N. Iwasa, S. Nagahama, T. Yamada and T. Mukai, Jpn. J. Appl. Phys. Lett. (34), L1332(1995)
2. T. Mukai, H. Niramatsu and S. Nakamura, Jpn. J. Appl. Phys. (37)L479(1998)
3. H. Amano, M. Kito, K. Hiramatsu and I. Akasaki, Jpn. J. Appl. Phys. (28) L2112. (1989)
4. S. Nakamura, T. Mukai and M. Senoh, Jpn J. Appl. Phys. (30)L1998(1991)
5. S. Nakamura, T. Mukai and M. Senoh, Appl. Phys. Lett. (64), 1687(1994)
6. S. Nakamura, M. Senoh, N. Iwasa and S Nagahama, Jpn. J Appl. Phys. Lett. (34), L797.(1995)
7. J. W. Yang, Q. Chen, C. J. Sun, B. Lim, M. Z. Anwar, M. A. Khan, H. Temkın, Appl. Phys. Lett. (69), 369 (1996)
8. S. Nakamura and G. Fasol, "The Blue Laser Diode", (Springer, Berlin 1997) p. 210
9. H. Kim, J. M. Lee, C. Huh, S. W. Kım, D. J. Kim, S. J. Park and H. Hwang, Appl. Phys. Lett. (77), 1903 (2000)
10. H. Ishikawa, S. Kobayashi, Y Koide, S. Yamasaki, S. Nagai, J. Umezaki, M Koike, and M. Murakami, J. Appl. Phys (81), 1315(1997)
11. A. Y. Polyakov, N. B. Smirnov, A. V Govorkov, A. S. Usikov, N. M. Shmidt and W. V. Lundin, Solid State Electron (45) 255-259 (2001)
12. A. Y. Polyakov, A . V. Govorkov, N. B. Smirnov, A. E. Nikolaev, I. P Nikitina, V. A. Dmitriev, Solid State Electron (45) 261-265 (2001)
13. H. Nakayama, P. Hacke, M. R. H. Khan, T. Detchprohm, K. Hiramatsu and N. Sawakı, Jpn. J. Appl. Phys. (35), L282-L284, (1996)
14. P. Kozodoy, A. Abare, R. K. Sink, M. Mack, S. Keller, S. P. DenBaars, U. K. Mishra and D. Steigerwald, Mat. Res. Soc. Symp. Proc. (468), 481 (1997)
15. S. Nakamura, Microelec. J. (25), 651 (1991)
16. M. E. Aumer, S. F. LeBoeuf, S. M. Bedair M. Smith, J. Y. Lin and H. X. Jiang, (77) 821 (2000)